A Primitive Enantiornithine Bird and the Origin of Feathers
Fucheng Zhang, *et al.*
Science **290**, 1955 (2000);
DOI: 10.1126/science.290.5498.1955

A Primitive Enantiornithine Bird and the Origin of Feathers

Fucheng Zhang* and Zhonghe Zhou

A fossil enantiornithine bird, *Protopteryx fengningensis* gen. et sp. nov., was collected from the Early Cretaceous Yixian Formation of Northern China. It provides fossil evidence of a triosseal canal in early birds. The manus and the alular digit are long, as in *Archaeopteryx* and *Confuciusornis*, but are relatively short in other enantiornithines. The alula or bastard wing is attached to an unreduced alular digit. The two central tail feathers are scalelike without branching. This type of feather may suggest that modern feathers evolved through the following stages: (i) elongated scale, (ii) central shaft, (iii) barbs, and finally (iv) barbules and barbicel.

Enantiornithine birds have generally been regarded as the most dominant birds in the Mesozoic (*1*–*4*). *Protopteryx*, the fossil bird described here, represents the most primitive enantiornithine and preserved many skeletal transitions from the most primitive birds *Archaeopteryx* and *Confuciusornis* to more advanced birds.

Discoveries of "fiber"-like structures in *Sinosauropteryx* (*5*), *Beipiaosaurus* (*6*), and *Sinornithosaurus* (*7*) and in two controversial feathered dinosaurs (*1*, *8*, *9*) have stimulated debates on the origin of feathers in addition to the origin of birds. Similarities have been found between the elongate integumentary appendages in the Late Triassic archosaur *Longisquama* and modern avian feathers (*10*). *Protopteryx* preserved some interesting types of feathers with characters between those of scales and modern feathers, thus providing fossil avian evidence for the origin of feathers from elongated scales in reptiles.

Protopteryx fengningensis is described as follows: Aves Linnaeus, 1758, Enantiornithes Walker, 1981, *Protopteryx fengningensis* gen. et sp. nov. Etymology: "*Protopteryx*" means primitive feather; "*fengningensis"* refers to the Fengning County where the specimens were collected. Holotype: A nearly completely articulated skeleton on the mainpart and counterpart slabs [Institute of Vertebrate Paleontology and Paleoanthropology (IVPP) collection number V 11665]. Paratype: A nearly completely articulated skeleton impression on the mainpart and counterpart slabs [IVPP collection number V 11844]. Horizon and locality: Yixian Formation, Early Cretaceous; Fengning County, Hebei Province, China. Diagnosis: Distal end of the minor metacarpal slightly passing the distal end of the major metacarpal. First phalanx of major digit shorter than the second phalanx. Second phalanx of minor digit small and triangular in shape. Coracoid with small procoracoid process; lateral process of coracoid prominent. Interclavicular angle 50°; hypocleideum about half the length of the clavicular ramus. Description: *Protopteryx* is about the size of a starling (*Sturnus cineraceus*), with feather imprints clearly preserved (Fig. 1A and Table 1).

In V 11665, the skull is partially crushed and the bones are disarticulated (Fig. 2A). In V 11844, only bone impressions are preserved. The snout is pointed; the orbit is large; the braincase is expanded. Teeth are present in the premaxilla and the dentary, as in most Mesozoic birds (*1*–*4*). A total of four teeth can be seen in V 11665. Two conical and unserrated teeth are associated with the premaxillae, probably one on each side. The other two teeth are preserved in the dentary; they are slightly subtriangular in shape; one is at the anterior end and the base appears to have a resorption pit, similar to that of *Archaeopteryx* (*11*); the other is approximately at the middle of the dentary. Two premaxillae are fused along the midline and possess long nasal processes, which extend to the lachrymal. The long quadrate lacks the orbital process as in *Archaeopteryx* and *Cathayornis* (Fig. 2, B to D). The robust postorbital is "Y"-shaped. It has a rodlike jugal process that probably contacts the jugal as in *Confuciusornis* (*12*) but is different from that of the Early Cretaceous bird from Spain (*13*).

The neck is composed of seven or eight cervical vertebrae, including the atlas and axis. The last cervical vertebra is slightly elongated. The number of dorsal vertebrae is 12. There are 14 dorsals in *Archaeopteryx* (*14*, *15*), 11 or 12 in *Confuciusornis*, and only about 11 in *Iberomesornis*. The neural spine of the dorsal vertebra is rectangular in shape and its length is about half that of the centrum. The synsacrum is composed of seven vertebrae; the neural spines of the sixth and seventh vertebrae are unified and can be well distinguished from that of the first caudal vertebra. The fifth through seventh vertebrae possess long transverse processes, and the transverse process of the sixth one is the longest, indicating tight contact with the ilium. There are six or seven free caudals. The neural spine of the first caudal vertebra is separate from that of the sixth and seventh sacral vertebrae. The transverse processes of the caudal vertebrae are shorter than those of the last three sacral vertebrae. The pygostyle is well fused and its total length is 11.3 mm, slightly longer than that of the free caudals.

There are 12 pairs of ribs preserved with the dorsal vertebrae. The first pair is short. The coracoid is elongated and strutlike. The ventral surface is flat and slightly convex near the sternal end. The dorsal side of the coracoid is concave, with small fossae and tubercles at the sternal half for the attachment of sternocorocoidal muscle, as in modern birds (*16*). Unlike other enantiornithines (*3*, *17*–*20*), the procoracoid process exists in *Protopteryx*. The lateral process is also more prominent than that of other enantiornithines (*20*) (Fig. 3, A and B). The scapular shaft is straight and becomes curved and thinner near the distal end. The coracoidal articulation is flat. The two clavicular rami form an angle of about 50°, which is smaller than that of *Concornis*. The acrocoracoid articular surface seems slightly expanded laterally. The hypocleideum is about half of the length of the clavicular ramus, with a small crest on the cranial side (Fig. 3, A and C). The caudal part of the sternum is notched, with two robust lateral processes and a triangular medial process. The medial carina extends along the posterior quarter of the ventral surface. The sternum appears to be as long as it is wide (Fig. 3, A and D).

The humerus is about the length of the ulna, with the capital groove well developed; the deltoid crest and external tubercle are well developed. The ulna is significantly broader and more robust than the radius. The radius is straighter than the ulna. The ratio of the shaft diameter of the ulna to the radius is about 2:1 (Fig. 4A). To avoid the controversy over the numbering of the metacarpals and manual digits in birds and dinosaurs, we follow the conventional terms (*16*) using alular, major, and minor, corresponding to "1, 2, 3" by some workers (*2*) and "2, 3, 4" by others (*1*). The manus is longer than the forearm (Fig. 4A). Two distal carpals are preserved; the bigger one (the semilunate bone) contacts the proximal ends of the alular and major metacarpals, and the smaller one contacts the proximal end of the minor metacarpal. The alular metacarpal is about 25% of the length of the major metacarpals. The major metacarpal is robust; the minor metacarpal is bow shaped and more slender than the major metacarpal; they are tightly attached to each

Institute of Vertebrate Paleontology and Paleoanthropology, Chinese Academy of Sciences, Post Office Box 643, Beijing 100044, China.

*To whom correspondence should be addressed. E-mail: fuchengzhang@yeah.net

other proximally but not fused, as shown by the suture between them. The intermetacarpal space between the major and minor metacarpals is narrow, similar to that of *Concornis*.

The alular digit bears two phalanges. The first phalanx is slender and long, and its distal end extends to the distal ends of the major and minor metacarpals; the ungual phalanx is shorter than that of the major digit. The major digit has three phalanges. The second phalanx is not reduced, and it is longer than the first phalanx, as in *Archaeopteryx* and *Confuciusornis* (*12*, *21*); whereas in other known enantiornithine birds, the second phalanx is shorter than the first one (*3*) (Fig. 4). The minor digit has two phalanges. The first phalanx is compressed; the ungual phalanx is triangular and small as compared with other unguals (Fig. 4).

The pubis is slender, elongated, and suboval in cross section. The distal end forms an expanded pubic foot. There exists a short pubic symphysis. The ischium is laminar; its proximal half is broad and tapers distally. Like *Archaeopteryx*, the ilium of *Protopteryx* has a wide and oval-shaped cranial part. The pre-acetabular portion is longer than the post-acetabular portion; the latter is more slender. The attachment of the ilium to the last three sacral vertebrae is tighter than to the other sacral vertebrae.

The femur is robust, slightly curved, and shorter than the tibiotarsus. The head and the trochanteric shelf are not separated by an obvious neck. The tibiotarsus is straight, and about 120% of the length of the femur. In medial view, the proximal end is semicircular, similar to that of *Archaeopteryx* (*21*). Two proximal tarsi contact the distal end of the tibia; the boundary between the astragalus and the calcaneum is obscured by damage, but its position is evident because of a shallow notch between the bones. There is one small separate distal tarsal at the proximal end of the metatarsals. The fibula is rodlike and long. Its proximal end is closely attached to the lateral side of the tibiotarsus; distally, it shifts from the lateral to the anterior side of the tibiotarsus.

The slightly curved second metatarsal lies medial to the distal end of the second. It is short and about a quarter of the length of metatarsal II. Metatarsals II through IV are straight throughout their length, although the distal end of metatarsal IV is slightly curved laterally. Metatarsals II through IV are fused only at their proximal ends. Among the three major metatarsals, metatarsal III is the longest. Its trochlea is narrower than that of metatarsal II, as in other enantiornithines. Metatarsal IV is slightly more slender than metatarsals II and III. Digit II is more robust than the other three. Digit IV is more slender than the other digits. The claws are long and curved.

Three types of feather can be identified. They are the flight feather (including the alula), the down feather, and the primitive, scalelike, central tail feathers. The body of *Protopteryx* was extensively covered by feathers, which were preserved as carbonized traces or structured imprints. The down feathers almost covered the whole body. The downs above the head are about 12.3 mm long and are shorter than those at the neck (which average 18.3 mm long). In the shoulder girdle, the feathers are 10 mm long on

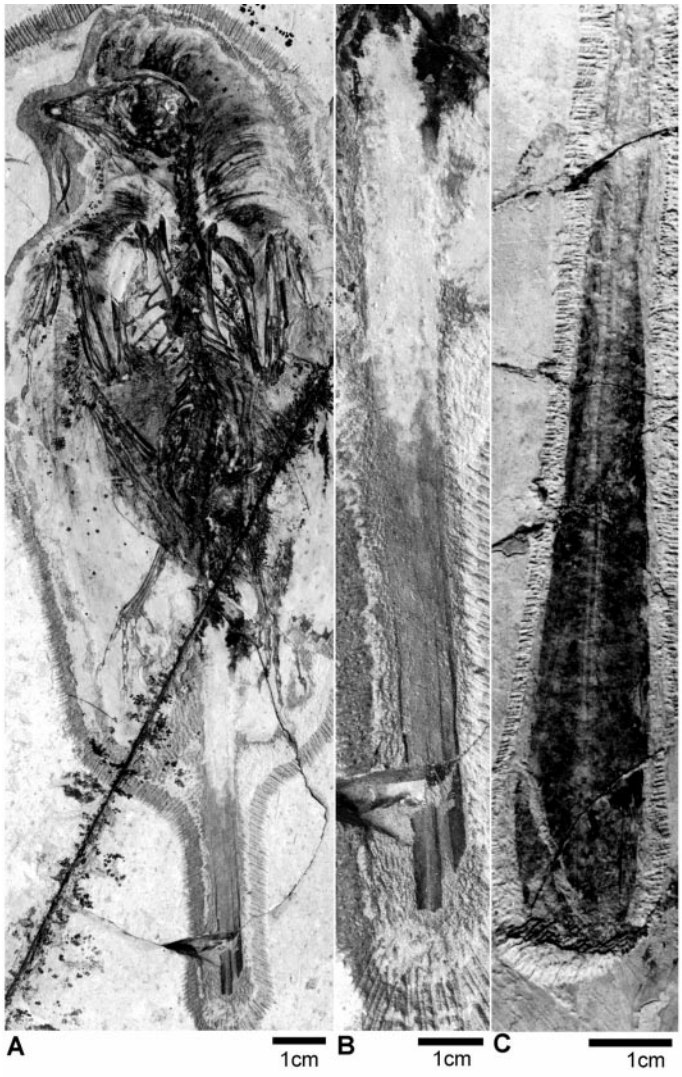

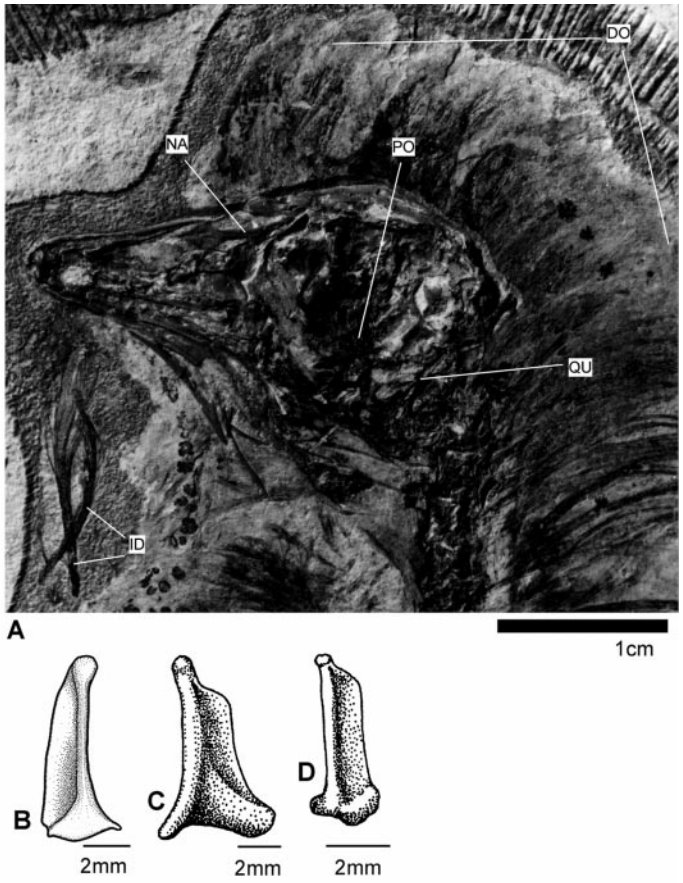

Fig. 1 (left). *Protopteryx fengningensis*. (**A**) Slab of *P. fengningensis* (V 11665). The skull is in left lateral view and the postcranial part is in ventral view. (**B**) The scalelike tail feather of *P. fengningensis* (V 11665). (**C**) The distal part of the central tail feather of *Confuciusornis*. **Fig. 2 (right).** The skull of *P. fengningensis*, holotype V 11665 (**A**) and comparisons of the quadrates in *P. fengningensis* (**B**), *Archaeopteryx* (**C**) [after (*37*)], and *Cathayornis* (**D**) [after (*37*)]. Abbreviations: DO, downfeathers; ID, isolated downfeathers; NA, nasal; PO, postorbit; and QU, quadrate.

average. The wing feathers seem less carbonized, as indicated by the light color and obvious traces. The maximum length of the wing feather is about 94 mm.

There are about two dozen barbs on an isolated down feather preserved near the head. The barbs are dispersed at the distal part and converged at the proximal part. At the proximal end of the shaft of the down, there is an afterfeather set off at an angle of about 45° with the rachis. Its barbs are laminar, not hairlike. There is no evidence of barbulae or hooklets. The wing flight feathers are asymmetric as in *Archaeopteryx*, Confuciusornis, and other flying birds. The two central tail feathers of *Protopteryx* are scalelike without barbs or rami at their proximal part (Fig. 1B).

Protopteryx possesses a combination of primitive and advanced characters [see (*22*)]. It shares with modern birds a procoracoid process and a lateral process of the coracoid. On the other hand, the long hand and alular digit, unfused carpometacarpus, and tibiotarsus are similar to those of *Archaeopteryx*. The character of the furcula, sternum, and carpometacarpus are all characteristic of enantiornithines. Compared with other known enantiornithines, *Protopteryx* appears to be more primitive in having an unreduced alular digit, unfused carpometacarpus, and unfused tibiotarsus (*22*).

In modern birds, the development of the procoracoid is an indicator of flight ability. Poor fliers such as pheasants have a reduced procoracoid. True fliers, such as perching birds and hawks, have a well-developed procoracoid. The base of the procoracoid and the adjacent part of the upper shaft of the coracoid form part of the sulcus supracoracoideus, a groove for the tendon of musculus supracoracoideus (*16*), which is the largest humeral abductor for the wing recovery stroke (*15*). Recent studies have found that the supracoracoideus tendon provides greater twisting force than elevating (perpendicular) force against the humerus in the nearly tangential orientation; the humeral rotation was key to the evolution of powered avian flight (*23*). The presence of the procoracoid together with the carina of the sternum, well-developed deltoid crest, and external tuberosity of the humerus suggest that *Protopteryx* may have developed modern bird–like musculus supracoracoideus and pectoralis.

The alula is the essential structure in modern birds for low-speed flight and maneuverability (*18*). The Early Cretaceous birds *Eoalulavis* from Spain and *Eoenantiornis* from China (*24*) have preserved the alula with a reduced alular digit. This feature, however, is absent in *Archaeopteryx* and *Confuciusornis*, in which the alular digit is unreduced with a large claw. *Protopteryx* still retains an unreduced alular digit, although the claw is relatively small (Fig. 4A).

Before the recent discoveries of feather or hairlike structures in theropod dinosaurs (*5*–*8*), feathers were regarded as a unique feature of birds (*25*, *26*). There are several competing hypotheses about the origin and early evolution of feathers. The major debate focuses on whether the feather evolved on an aerodynamic background (*1*, *27*, *28*) or a nonaerodynamic background, such as for purposes of insulation, weight reduction (*29*), heat shields (*30*), waterproofing (*25*), or display (*31*).

The oldest bird, *Archaeopteryx*, does not provide much information about the origin of feathers because its feathers are almost identical to those of living birds (*32*). The association of the hairlike structures of small theropod dinosaurs with feather origins is based on three known theropods, including *Sinosauropteryx*, *Beipiaosaurus*, and *Sinornithosaurus* (*5*–*7*), yet there is no convincing evidence that they are branched. More work needs to be done to reveal their implications for the evolution of the origin of feathers in birds. The recent discoveries of true avian feathers in *Caudipteryx* and *Protarchaeopteryx* have been regarded by many as the strong evidence for the presence of feathered dinosaurs (*8*, *9*); however, some believe that *Caudipteryx* could be a secondarily flightless bird, and therefore the feathers in *Caudipteryx* were also secondarily reduced (*1*, *33*). Because *Caudipteryx* is generally believed to be closely related to oviraptorids (*9*, *34*), which are less closely related to birds than to dromaeosaurs such as *Sinornithosaurus* that possessed hairlike structures, it is therefore uncertain whether the feathers in *Caudipteryx* were independently developed or were the primitive type of feathers defining birds and their immediate ancestors. The similarities between the nonavian "feathers" in *Longisquama* and modern avian feathers suggest that the earliest stages of the evolution of avian feathers were more complex than we have expected (*10*).

Protopteryx retains a feather type that has never before been described: It lacks barbs or rami at the proximal end. In V 11665, two long central tail feathers are preserved. Their proximal ends are attached to the pygostyle, and the distal ends are missing. The distal ends of the tail feathers were broken cleanly before burial. The break in the right tail feather was perpendicular to the long axis and shows no sign of splitting or fraying. The uniform nature of the break would not be expected if barbs and barbules were present (*30*). In V 11844, the proximal end of the tail feathers also remains unified without branching. It is noteworthy that this kind of feather is also present in some *Confuciusornis* (*35*) and other undescribed enantiornithines. At the distal part, there is a undifferentiated vane region between the central rachis and outer branched barbs. Such a feather structure, including those of some long tail feathers of *Confuciusornis* (Fig. 1C) and at least four other enantiornithines, is different from those of all other known fossil and modern feathers.

In a few modern birds such as the red bird of paradise (*Paradisaea rubra*), the central tail looks like strips of plastics (*36*) and has undifferentiated vanes, similar to the situation in *Protopteryx* and *Confuciusornis*. One explanation is that this feather structure is primitive, and its presence in birds of paradise is neotenic. Modern feathers probably evolved through the following stages: (i) elongation of scales, (ii) appearance of a central shaft, (iii) differentiation of vanes into barbs, and (iv) appearance of barbules and barbicel. However, *Protopteryx* is undoubtedly younger and more advanced than *Ar-*

Table 1. Measurements of *P. fengningensis* (in millimeters).

	V 11665	V 11844
Skull length	28.3	–
Neck length	18.5	19.1
Dorsal vertebra length	33.9	34.0
Tail length	20.7	21.4
Scapula length	21.7	–
Sternum length	–	15.9
Sternum width	–	16.9
Coracoid length	–	12.7
Furcula total length	14.7	14.0
Wing length	85.5	85.9
Ilium length	15.3	14.8
Ischium length	12.9	–
Pubis length	22.3	–
Hindlimb length	86.3	–
Isolated down feather length 1	14.9	–
Isolated down feather length 2	11.8	–
Maximum length of wing flight feather	94.0	–
Preserved central tail feather length	77.0	–
Tail feather width at the break point	2.1	–
Tail feather width at the proximal half	–	2.3

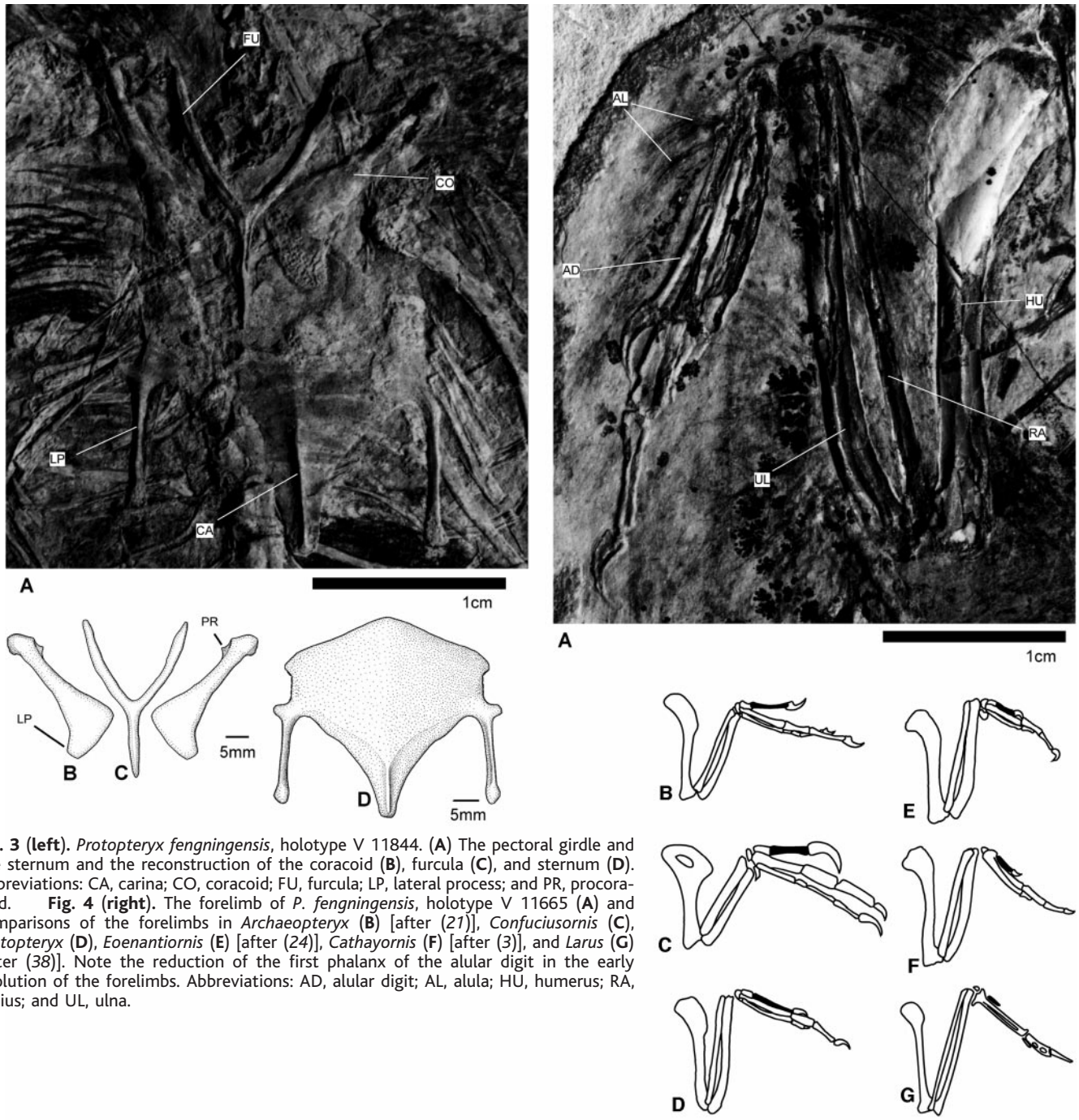

Fig. 3 (left). *Protopteryx fengningensis*, holotype V 11844. (**A**) The pectoral girdle and the sternum and the reconstruction of the coracoid (**B**), furcula (**C**), and sternum (**D**). Abbreviations: CA, carina; CO, coracoid; FU, furcula; LP, lateral process; and PR, procoracoid. **Fig. 4 (right).** The forelimb of *P. fengningensis*, holotype V 11665 (**A**) and comparisons of the forelimbs in *Archaeopteryx* (**B**) [after (*21*)], *Confuciusornis* (**C**), *Protopteryx* (**D**), *Eoenantiornis* (**E**) [after (*24*)], *Cathayornis* (**F**) [after (*3*)], and *Larus* (**G**) [after (*38*)]. Note the reduction of the first phalanx of the alular digit in the early evolution of the forelimbs. Abbreviations: AD, alular digit; AL, alula; HU, humerus; RA, radius; and UL, ulna.

chaeopteryx, and therefore an alternative explanation of this feather type in *Protopteryx* is that it was secondary specialization from its ancestral normal feathers. In any case, flight and down feathers may have differentiated separately from the elongated nonshafted scales in the early stage of the evolution of feathers.

References and Notes

1. A. Feduccia, *The Origin and Evolution of Birds* (Yale Univ. Press, New Haven, CT, ed. 2, 1999), pp. 1–405.
2. L. M. Chiappe, *Nature* **378**, 349 (1995).
3. Z. Zhou, *Cour. Forchungsinst. Senckenb.* **181**, 9 (1995).
4. K. Padian, L. M. Chiappe, *Biol. Rev.* **73**, 1 (1998).
5. P. Chen, Z. Dong, S. Zhen, *Nature* **391**, 147 (1998).
6. X. Xu, Z. Tang, X. Wang, *Nature* **399**, 350 (1999).
7. X. Xu, X. Wang, X. Wu, *Nature* **401**, 262 (1999).
8. Q. Ji, P. J. Currie, M. A. Norell, S. Ji, *Nature* **393**, 753 (1998).
9. Z. Zhou, X. Wang, *Vertebr. Palasiat.* **38**, 111 (2000).
10. T. D. Jones *et al.*, *Science* **288**, 2202 (2000).
11. L. D. Martin, J. D. Stewart, K. Whetstone, *Auk* **97**, 86 (1980).
12. L. Hou, L. D. Martin, Z. Zhou, A. Feduccia, F. Zhang, *Nature* **399**, 679 (1999).
13. J. L. Sanz *et al.*, *Science* **276**, 1543 (1997).
14. P. Wellnhofer, *Palaeontographica* **147**, 169 (1974).
15. J. H. Ostrom, *Smithson. Contrib. Paleobiol.* **27**, 1 (1976).
16. J. J. Baumel, L. M. Witmer, in *Handbook of Avian Anatomy: Nomina Anatomica Avium*, J. J. Baumel, Ed. (Publication 23, Nuttall Ornithology Club, Cambridge, MA, ed. 2, 1993), pp. 45–132.
17. L. D. Martin, *Cour. Forchungsinst. Senckenb.* **181**, 23 (1995).
18. J. L. Sanz *et al.*, *Nature* **382**, 442 (1996).
19. L. M. Chiappe, in *Münchner Geowiss. Abh. A 30*, G. Arratia, Ed. (Munich, Germany, 1996), pp. 203–244.
20. C. A. Walker, *Nature* **292**, 51 (1981).
21. P. Wellnhofer, in *Proceedings of the II International Symposium of Avian Paleontology and Evolution*, K. E. Campbell, Ed. (Papers in Avian Paleontology Honoring Pierce Brodkorb, Natural History Museum of Los Angeles, Los Angeles, CA, 1992), pp. 3–23.
22. Supplementary Web material is available on *Science* Online at www.sciencemag.org/cgi/content/full/290/5498/1955/DC1.
23. J. H. Ostrom, *Dinofest Intern. Proc.* **1997**, 301 (1997).

24. L. Hou, L. D. Martin, Z. Zhou, A. Feduccia, *Vertebr. Palasiat.* **37**, 88 (1999).
25. J. Dyck, *Zool. Scr.* **14**, 137 (1985).
26. H. B. Ginn, D. S. Melville, *British Trust for Ornithology Guide 19* (Maund & Irvine, Tring, Hertfordshire, UK, 1983), pp. 1–112.
27. W. J. Bock, *Mem. Calif. Acad. Sci.* **8**, 57 (1986).
28. J. H. Ostrom, *Quart. Rev. Biol.* **49**, 27 (1974).
29. A. M. Lucas, P. R. Stettenheim, *Avian Anatomy: Integument* (Agricultural Handbook 362, U.S. Government Printing Office, Washington, DC, 1972), pp. 1–750.
30. P. J. Regal, *Quart. Rev. Biol.* **50**, 35 (1975).
31. E. Mayr, in *The Evolution of Life*, S. Tax, Ed. (Univ. of Chicago Press, Chicago, IL, 1960), pp. 349–380.
32. P. J. Griffiths, *Archaeopteryx* **14**, 1(1996).
33. T. D. Jones, J. O. Farlow, J. A. Ruben, D. H. Henderson, W. J. Hillenius, *Nature* **406**, 716 (2000).
34. P. C. Sereno, *Science* **284**, 2137 (1999).
35. L. M. Chiappe, S. Ji, Q. Ji, M. A. Norell, *Bull. Am. Mus. Nat. Hist.* **242**, 1 (1999).
36. F. B. Gill, *Ornithology* (Freeman, New York, 1994), pp. 65–113.
37. L. D. Martin, Z. Zhou, *Nature* **389**, 556 (1997).
38. R. W. Storer, in *Proceedings of the XII International Ornithological Congress* (Helsinki, 1960), pp. 694-707.
39. We thank G.-M. Zheng, L.-H. Hou, M.-M. Chang, W. Gao, X.-C. Wu, P. G. P. Ericson, F. Jin, J.-S. Dong, J.-Y. Zhang, Y.-Q. Wang, P.-F. Chen, X.-L. Wang, Y.-M. Hu, H.-L. You, Y. Wang, and X. Xu for discussions and reading the manuscript and Y.-T. Li, J. Zhang, and Z.-L. Tang for technical support. Supported by the Special Funds for Major State Basic Research Projects of China (grant G2000077700), the Chinese Academy of Sciences (CAS) (grants KZ951-B1-410, KZCX3-J-03, and 9910), the National Natural Science Foundation of China (grants 40002002 and J9930095), the U.S. National Geographic Society, the "Hundred Talents Project" of the CAS to Z.-H.Z., and the Fengning County Government.

9 June 2000; accepted 6 November 2000

Glucose-Dependent Insulin Release from Genetically Engineered K Cells

Anthony T. Cheung,[1,3] Bama Dayanandan,[1] Jamie T. Lewis,[1] Gregory S. Korbutt,[2] Ray V. Rajotte,[2] Michael Bryer-Ash,[4] Michael O. Boylan,[5] M. Michael Wolfe,[5] Timothy J. Kieffer[1,3]*

Genetic engineering of non-β cells to release insulin upon feeding could be a therapeutic modality for patients with diabetes. A tumor-derived K-cell line was induced to produce human insulin by providing the cells with the human insulin gene linked to the 5′-regulatory region of the gene encoding glucose-dependent insulinotropic polypeptide (GIP). Mice expressing this transgene produced human insulin specifically in gut K cells. This insulin protected the mice from developing diabetes and maintained glucose tolerance after destruction of the native insulin-producing β cells.

Diabetes mellitus (DM) is a debilitating metabolic disease caused by absent (type 1) or insufficient (type 2) insulin production from pancreatic β cells. In these patients, glucose control depends on careful coordination of insulin doses, food intake, and physical activity and close monitoring of blood glucose concentrations. Ideal glucose levels are rarely attainable in patients requiring insulin injections (*1*). As a result, diabetic patients are presently still at risk for the development of serious long-term complications, such as cardiovascular disorders, kidney disease, and blindness.

A number of studies have addressed the feasibility of in vivo gene therapy for the delivery of insulin to diabetic patients. Engineering of ectopic insulin production and secretion in autologous non-β cells is expected to create cells that evade immune destruction and to provide a steady supply of insulin. Target tissues tested include liver, muscle, pituitary, hematopoietic stem cells, fibroblasts, and exocrine glands of the gastrointestinal tract (*2*–*7*). However, achieving glucose-dependent insulin release continues to limit the clinical application of these approaches. Some researchers have attempted to derive glucose-regulated insulin production by driving insulin gene expression with various glucose-sensitive promoter elements (*8*). However, the slow time course of transcriptional control by glucose makes synchronizing insulin production with the periodic fluctuations in blood glucose levels an extremely difficult task. The timing of insulin delivery is crucial for optimal regulation of glucose homeostasis; late delivery of insulin can lead to impaired glucose tolerance and potentially lethal episodes of hypoglycemic shock. Therefore, what is needed for insulin gene therapy is a target endocrine cell that is capable of processing and storing insulin and of releasing it in such a way that normal glucose homeostasis is maintained.

Other than β cells, there are very few glucose-responsive native endocrine cells in the body. K cells located primarily in the stomach, duodenum, and jejunum secrete the hormone GIP (*9*, *10*), which normally functions to potentiate insulin release after a meal (*11*). Notably, the secretion kinetics of GIP in humans closely parallels that of insulin, rising within a few minutes after glucose ingestion and returning to basal levels within 2 hours (*12*). GIP expression (*13*) and release (*14*) have also been shown to be glucose-dependent in vitro. However, the mechanism that governs such glucose-responsiveness is unclear. We made an interesting observation of glucokinase (GK) expression in gut K cells (Fig. 1A). GK, a rate-limiting enzyme of glucose metabolism in β cells, is recognized as the pancreatic "glucose-sensor" (*15*). This observation raises the possibility that GK may also confer glucose-responsiveness to these gut endocrine cells. Given the similarities between K cells and pancreatic β cells, we proposed to use K cells in the gut as target cells for insulin gene therapy.

A GIP-expressing cell line was established to investigate whether the GIP promoter is effective in targeting insulin gene expression to K cells. This cell line was cloned from the murine intestinal cell line STC-1, a mixed population of gut endocrine cells (*16*). K cells in this population were visually identified by transfection of an expression plasmid containing ~2.5 kb of the rat GIP promoter fused to the gene encoding the enhanced green fluorescent protein (EGFP) (*17*). After clonal expansion of the transiently fluorescent cells, clones were analyzed for the expression of GIP mRNA by Northern blotting (*18*). The amount of GIP mRNA in one clone (GIP tumor cells; GTC-1) was ~8 times that in the parental heterogeneous STC-1 cells (Fig. 1B). Transfection of GTC-1 cells with the human genomic preproinsulin gene linked to the 3′ end of ~2.5 kb of the rat GIP promoter (Fig. 1C, GIP/Ins) resulted in a correctly processed human preproinsulin mRNA transcript (*19*) (Fig. 1D). When the same GIP/Ins construct was transfected into a β-cell line (INS-1), a liver cell line (HepG2), and a rat fibroblast (3T3-L1) cell line, little human preproinsulin mRNA was detectable (*20*). These observations suggest that the GIP promoter used is cell-specific and is likely to be effective in targeting transgene expression specifically to K cells in vivo. Western blot analysis revealed that the proprotein convertases required for correct processing of proinsulin to mature insulin (PC1/3 and PC2) (*21*) were expressed in GTC-1 cells (Fig. 1E) (*22*). Consistent with this observation, a similar molar ratio of human insulin and C pep-

[1]Departments of Medicine and Physiology, and [2]Department of Surgery, University of Alberta, Edmonton, AB T6G 2S2, Canada. [3]enGene, Inc., Edmonton, AB T6G 2T5, Canada. [4]Department of Medicine, University of Tennessee, Memphis, TN 38103, USA. [5]Section of Gastroenterology, Boston Medical Center, Boston, MA 02118, USA.

*To whom correspondence should be addressed. E-mail: tim.kieffer@ualberta.ca